Food Science and Biotechnology
https://doi.org/10.1007/s10068-026-02351-1

RESEARCH ARTICLE

Spray drying process optimization for encapsulation of *Lactobacillus acidophilus* in autolyzed yeast cell-based microcapsules: structural and functional evaluation

Ilyas Atalar[1] · Sibel Yılmaz[1] · Tahra El-Obeid[2] · Muhammet İrfan Aksu[3] · Ömer Said Toker[4] · Şirin Oba İlter[5] · Abdullah Kurt[4] · Nevzat Konar[6]

Received: 9 May 2026 / Revised: 20 September 2026 / Accepted: 15 October 2026
© The Korean Society of Food Science and Technology 2026

Abstract

This study investigated the efficacy of spray-drying microencapsulation using autolyzed yeast cells (AYC) as a novel wall material to protect *Lactobacillus acidophilus*. Process parameters directly governed cell survival, yielding survival rates between 59.46% and 82.15%, with the maximum recovery achieved at 135 °C and 10% solids. Free cells suffered severe mortality during in vitro digestion, declining sharply from 9.30 ± 0.06 to 1.22 ± 0.07 log CFU/mL in gastric fluid and 0.52 ± 0.03 log CFU/mL in intestinal fluid. Conversely, AYC microcapsules produced under multi-response optimized conditions exhibited 7.24 ± 0.11 log CFU/mL post-drying, retained 5.25 ± 0.12 log CFU/mL after sequential intestinal transit, and maintained 5.51 ± 0.18 log CFU/mL following 90 days of refrigerated storage. SEM and FTIR characterizations confirmed the formation of intact spherical microcapsules and a marked increase in rigid β-sheet protein conformations. AYC represents a sustainable, high-performance carrier for delivering viable probiotics through gastrointestinal stress.

Keywords *Lactobacillus acidophilus* · Autolyzed yeast cell · Microencapsulation · Spray drying · Gastrointestinal stability

Introduction

The integration of probiotics, specifically *Lactobacillus acidophilus*, into functional food systems remains a significant challenge due to their high sensitivity to environmental stressors. Microencapsulation has emerged as a critical biophysical strategy to safeguard these probiotics, enhancing their viability during industrial processing, long-term storage, and transit through the rigorous gastrointestinal environments (Rajam & Anandharamakrishnan, 2015). This method, by establishing a protective shield, reduces the vulnerability of sensitive microbial cells to harmful external factors, thereby facilitating the delivery of a therapeutic dose of viable probiotics to the host's gastrointestinal tract, where they can confer their desired health benefits (Vivek et al., 2023). Spray drying, a prevalent encapsulation technology within food technology, is favored for its economic viability, substantial production capacity, and adaptability. This process generally produces microcapsules ranging from 10 to 100 μm in diameter, dimensions that are well-suited for effortless integration into diverse food matrices (Ngoc Le & Chen, 2025). Conversely, the efficacy of spray drying depends on careful selection of wall materials and meticulous optimization of process parameters, such as inlet temperature, feed flow rate, and nozzle diameter (Yu et al., 2024). Under challenging conditions, these materials must provide physical protection while maintaining the structural integrity of the microcapsules (Firdaus et al., 2025). The selection of the encapsulation matrix is the primary

✉ Ilyas Atalar
ilyas.atalar@ogu.edu.tr

1 Agriculture Faculty, Food Engineering Department, Eskisehir Osmangazi University, Eskisehir, Turkey

2 QU Health, College of Health Sciences, Department of Nutrition Sciences, Qatar University, Doha, Qatar

3 Agriculture Faculty, Food Engineering Department, Ataturk University, Erzurum, Turkey

4 Faculty of Chemical and Metallurgical Engineering, Food Engineering Department, Yıldız Technical University, Istanbul, Turkey

5 Suluova Vocational School, Department of Food Processing, Amasya University, Amasya, Turkey

6 Agriculture Faculty, Dairy Technology Department, Ankara University, Ankara, Turkey

Published online: 25 October 2026

determinant of survival and stability for sensitive organisms such as *L. acidophilus* (Guo et al., 2022). Autolyzed yeast cell (AYC) is a novel wall material that is both sustainable and promising in this context. β-D-glucans are abundant in AYC, which contribute to its inherent structural integrity and distinctive prebiotic properties (Borchani et al., 2016; Kayanna et al., 2022). In addition to their role as a physical barrier, β-D-glucans can selectively stimulate the proliferation of advantageous *Lactobacillus* species, thereby establishing a synbiotic microenvironment within the capsule (Kayanna et al., 2022). The viscosity and flow properties of the feed, both crucial for stable microcapsule formation, are significantly influenced by the molecular weight and branching degree of these polysaccharides (Kayanna et al., 2022). Furthermore, the carbohydrate-protein complex found within the yeast cell biomass demonstrates enhanced emulsifying capabilities and oxidative stability, facilitating the creation of microcapsules with smooth surface morphologies and improved resistance to thermal and acidic stress (Synytsya & Novák, 2013; Younesi et al., 2023). Ahmadi et al. (2025) investigated the enhanced survival of *L. acidophilus* via spray-drying encapsulation, using yeast cell wall (YCW) or β-D-glucans as supplementary coating agents in combination with a sodium alginate matrix. While sodium alginate is a frequently employed biocompatible carrier, it often demonstrates burst release at low pH levels due to matrix degradation, leading to premature probiotic exposure. The microcapsules, prepared with alginate and 3% YCW, maintained a significant concentration of 8.77 log CFU/mL after 480 min, demonstrating improved structural protection under simulated conditions; in contrast, free cells lost viability completely within 240 min. Furthermore, the research indicated that the specific death rate at 25 °C was significantly lower for Alg-Y3 (0.0988 day^{-1}) than for pure alginate (0.3375 day^{-1}). This indicates that the inclusion of YCW slows the probiotic's inhibition rate by more than 3-fold. Günal-Köroğlu et al. (2024) investigated the core methodologies and key outcomes of employing yeast cells as natural microencapsulation agents for sensitive bioactive substances, particularly hydrophobic molecules. Their study highlights yeast-based encapsulation as an economically viable, environmentally friendly, and straightforward method for protecting fragile compounds from environmental degradation, thereby improving their stability in food matrices and enhancing their bioavailability in the gastrointestinal system. Despite the potential of yeast-derived components, a comprehensive evaluation of their effectiveness as primary encapsulating agents for probiotics remains lacking. This study aimed to rectify this gap by exploring the use of autolyzed yeast cell biomass in the spray-drying microencapsulation of *L. acidophilus*. Our investigation centers on optimizing the spray-drying procedure and comprehensively characterizing the resultant microcapsules, including structural morphology and protective performance under simulated gastrointestinal conditions and during extended storage. To the best of our knowledge, this study represents the first systematic evaluation of the structural and functional interplay between autolyzed yeast cells and *L. acidophilus*, offering novel perspectives on the development of resilient, sustainable probiotic delivery systems for functional food technology.

Materials and methods

Preparation of autolyzed and dried *Saccharomyces cerevisiae* biomass

Food-grade autolyzed and dried *Saccharomyces cerevisiae* biomass originating from the reference strain NCYC-R-625 (registered at the National Collection of Yeast Cultures, Norwich, UK) was obtained from Pakmaya (As Gıda A.Ş., Kocaeli, Türkiye). Based on standard technical specifications, the autolyzed yeast biomass typically contains approximately 45–50% crude protein, 30–35% total carbohydrates (predominantly cell wall β-glucans and mannans), 5–8% ash, and 4–6% moisture. To prepare the wall material stock dispersion, the dried autolyzed yeast cell (AYC) biomass was reconstituted in deionized water ($30.0g/100mL$) under continuous mechanical agitation. The solution was heated to 80 °C and maintained at this temperature for 2 h under gentle stirring. This thermal hydration step was performed to fully inactivate any residual endogenous yeast proteases and nucleases while promoting hydration, structural swelling, and extraction of cell wall β-D-glucans and mannoprotein complexes, which are essential for film formation during microencapsulation. Following thermal hydration, the drying was performed out using the spray-drying method. Spray drying was done in a lab-scale spray dryer (B290, Buchi, Fluwil, Switzerland). For the process, an autolyzed and dried *S. cerevisiae* NCYC-R-625 solution (15.0 g/100 mL) was prepared. Drying conditions were 6 bar gas pressure, 1.40 mL min^{-1} flow, and 65 mbar atomization pressure. Because this precursor matrix contained no living biological cells, high drying temperatures were applied to maximize thermal drying efficiency and moisture removal: inlet air temperature of 180 °C, outlet air temperature of 100 °C, feed flow rate of $1.40mL/min$, atomization gas pressure of 6 bar, and aspirator flow rate of $35m^3/h$ ($65mbar$ pressure drop). The resultant dry AYC powder ($a_w < 0.15$) was sealed in air-tight, light-barrier containers and stored at $20.0 \pm 2.0°C$ until feed preparation (ElObeid et al., 2025). The probiotic *Lactobacillus acidophilus* strain LA-5 was supplied in lyophilized form by MAYSA Gıda San. ve Tic. A.Ş. (Tuzla, Istanbul, Türkiye).

Use of autolyzed yeast cell walls in probiotic microencapsulation

The encapsulation feed was prepared by dispersing autolyzed yeast cells (AYC) in deionized water at concentrations defined by the experimental design (10–30%, w/v). This mixture was stirred continuously to ensure a homogeneous suspension, and the concentrated *L. acidophilus* biomass was added. The final feed suspension was maintained under continuous gentle agitation using a magnetic stirrer throughout the spray-drying process to ensure uniform atomization and prevent yeast cell settling. A Face-Centered Central Composite Design was created to optimize spray-drying encapsulation process conditions and to reveal their effects on viability after drying, in vitro digestion, and storage. Based on preliminary trials and literature research, air inlet temperature (120–150 ℃), coating concentration (10–30%), and pump speed (6–14 mL/min) were selected as independent parameters (Supplementary File 1).

Bacterial enrichment, counting and calculating the survival rate

The bacterial enrichment process was performed according to the method described by Amiri et al. (2019). To enrich bacteria, 0.5 g of *L. acidophilus* was added to 5 mL of MRS liquid medium and incubated at 37 °C under aerobic conditions for 24 h. The resulting cultures were subcultured with 95 mL of MRS liquid medium and incubated under the same conditions for 24 h. To collect the biomass, the cultures were centrifuged at 4 °C at 4000 × g for 10 min, and the supernatant was removed. The cells were washed twice with sterile, isotonic NaCl solution, centrifuged again, and resuspended in isotonic NaCl to obtain a suspension containing 9–10 log CFU/mL for microencapsulation. To prepare the encapsulation feed, the pre-dried AYC powder was re-dispersed in sterile deionized water at the solid concentrations prescribed by the Face-Centered Central Composite Design experimental design (10%, 20%, or 30%w/v) and stirred for 1 h to ensure complete hydration. The concentrated *L. acidophilus* LA-5 suspension was then introduced into the AYC slurry at a fixed volumetric ratio of $1:9(v/v)$ (i.e., $10mL$ of bacterial concentrate per $90mL$ of AYC solution), yielding an initial viable cell load (N_0) of approximately $9.30 logCFU/mL$ across all formulations. The final slurry was held under gentle, continuous magnetic stirring during the encapsulation process to maintain suspension homogeneity and prevent settling. In contrast to the initial carrier powder preparation (180 °C), encapsulation drying was operated at milder inlet temperatures ($120-150°C$), corresponding to outlet temperatures of $45-84°C$, which are required to safeguard probiotic viability from lethal thermal denaturation during moisture evaporation. Bacterial counts were performed using MRS Agar (Merck, Germany) for *L. acidophilus* strains. Peptone water was used for dilutions, and the pour plate method was applied. After incubating the petri dishes at 37 °C for 72 h, the results were expressed as colony-forming units (log CFU/mL). To determine the survival rate (SR), the method of Semyonov et al. (2011) was followed. A 0.1 g sample of the spray-dried capsules was dissolved in 9.9 mL of phosphate buffer using a magnetic stirrer for 10 min. Serial dilutions were prepared in 0.1% peptone water, and viable cell counts were determined by the pour plate method on MRS agar. Survival rate was calculated using the following equation (Eq. 1)

$$Survivalrate(\%) = 100x\frac{\log N}{\log N_0} \quad (1)$$

where N_0 represents the viable count before drying (CFU/mL) and N represents the count after drying (CFU/ mL).

Determination of in vitro simulated gastrointestinal viability of encapsulated probiotic bacteria

The in vitro simulated digestion analysis of encapsulated probiotic bacteria was performed according to the protocol of Brodkorb et al. (2019). This protocol aims to simulate the processes of oral, gastric, and intestinal digestion. For the oral digestion simulation, 1 g of encapsulated *L. acidophilus* was mixed with salivary fluid (3.5 mL), α-amylase solution (0.5 mL), $CaCl_2$ (25 µL), and distilled water (975 µL). After adjusting the pH of the mixture to 7.0 with 1 mol/L NaOH, it was incubated at 37 °C for 2 min. After oral digestion was complete, the mixture was mixed with gastric fluid (6 mL), pepsin solution (1.28 mL), distilled water (556 µL), and $CaCl_2$ (4 µL) for gastric digestion simulation, and the pH was adjusted to 3.0 with 1 mol/L HCl. The mixture was incubated at 37 °C for 2 h. A 1 mL sample was taken from the simulated gastric environment, and the viability of the encapsulated probiotic bacteria after gastric digestion was determined using the pour plate method. After gastric digestion was complete, the mixture was mixed with intestinal fluid (7.7 mL), pancreatin solution (3.5 mL), bile solution (1.75 mL), distilled water (917 µL), and $CaCl_2$ (28 µL) for intestinal digestion simulation. The pH of the mixture was adjusted to 7.0 with 1 mol/L NaOH, and the mixture was incubated at 37 °C for 2 h. Then, a 1 mL sample was taken from the simulated intestinal environment, and the viability of the encapsulated probiotic bacteria after intestinal digestion was determined using the pour plate method.

Determination of the storage stability of encapsulated probiotic bacteria

To evaluate shelf life, the capsules were stored at 4 °C for 90 days in high-density polyethylene bottles. Live counts were performed at 0, 30, 60, and 90 days by dissolving the

capsules in phosphate buffer and incubating them on MRS agar at 37 °C for 72 h.

Dry matter content

Encapsulated powders were placed in stainless steel containers in specific amounts and kept in an oven (FN 300, Nüve, Turkey) at 105 °C until a constant weight. After this process, the containers were placed in a desiccator, and once cooled, the final sample weights were measured. When a constant weight was reached, the percentage (%) of dry matter was calculated.

Water activity

Water activity (a_w) of encapsulated dried probiotic *Lactobacillus acidophilus* was measured using a Water Lab water activity analyzer (Steroglass, Umbria, Italy).

Determination of optimal process conditions

The effect of each factor on the techno-functional, structural, and physicochemical properties was determined using ANOVA in Design-Expert Trial 13.0, with the experimental design generated via Face-Centered Central Composite Design. Optimum points were determined for minimum water activity, maximum dry matter, maximum viability after drying, and after digestion, and after 90 days of storage. The conditions that showed the highest desirability were used for the SEM, FTIR, and heat stability tests of the material.

Microstructure (SEM)

The microstructure of the capsules was also determined using a scanning electron microscope (JSM-7001F Jeol Japan). The samples were coated with a 10 nm thick gold–palladium layer (Quorum SC7620, UK). Images were obtained at 500, 1000, and 2000× magnification.

Determination of secondary structure by FT-IR spectra

Encapsulated probiotics in powder form were analyzed by FTIR (Bruker, Alpha II, Ettlingen, Germany) to investigate changes in chemical bond structures. The measurements were performed in Attenuated Total Reflection (ATR) mode, enabling direct analysis of the powder samples without further preparation. For this purpose, powder samples were analyzed in the wavelength range of 4.000–500 cm^{-1} and with a resolution of 4 cm^{-1}. To specifically evaluate the impact of the encapsulation process, FTIR analysis was conducted on both the control group (autolyzed yeast cells before spray drying) and the optimized microcapsule formulation (derived from the RSM results). Detailed investigations of amide groups were performed by taking second derivatives from the data. In addition, α-helix, β-sheet, β-turn, and random coil structures were examined in detail using FTIR spectroscopy. The secondary structure of the protein was determined using the characteristic absorption band in the amide I region (1600–1700 cm^{-1}). Quantitative analysis of the amide I band was performed using Peakfit 4.12 software (Systat Software, Inc., San Jose, USA). The baseline-corrected spectra were deconvoluted using Gaussian functions to separate individual subpeaks. The assignment of subpeaks to specific secondary structures was performed according to the following frequency ranges: β-sheet: 1615–1637 cm^{-1} and 1682–1700 cm^{-1}; Random coil: 1637–1648 cm^{-1}; α-helix: 1648–1664 cm^{-1}; β-turn: 1664–1681 cm^{-1} (Zhang et al., 2022). The relative percentage of each secondary structure was calculated by dividing the integral area of the assigned sub-peaks by the total area of the Amide I band.

Heat stability

To determine the viability of encapsulated probiotics in powder form at different temperatures, 10 mg of the probiotics were diluted in 5 mL of distilled water for the heat-stability test. Microencapsulated cells in sterile test tubes were heated in a water bath at 3 temperatures (65 °C, 75 °C, and 85 °C) for 1, 2, and 3 min, respectively. The selection of time–temperature combinations was designed to simulate a range of common industrial thermal treatments used in the production of functional foods. Cell viability of the samples before and after heating was determined using the pour plate technique on MRS agar. Petri dishes were incubated at 37 °C for 72 h. The resulting colonies were counted and recorded as log CFU/mL.

Statistical analysis

The Face-Centered Central Composite Design was used to plan 16 experimental runs, as shown in Supplementary File 1. The design was used to examine the effects of inlet air temperature (120–150), wall material concentration (10–30%) and pump rate (6–14 mL/min). Statistical significance for both the Analysis of Variance (ANOVA) and the Response Surface Methodology (RSM) was consistently evaluated at the 95% confidence level ($p < 0.05$). Factors with $p < 0.05$ were considered statistically significant, whereas those with $0.05 \leq p < 0.10$ were designated as showing a statistical trend toward significance. This uniform threshold was applied to assess the significance of the developed predictive models, individual process parameters

(inlet temperature, concentration, and pump rate), and their interactions. The adequacy of these models was further confirmed by the non-significant Lack-of-Fit results ($p > 0.05$) across all studied responses. The models were then used to identify optimal conditions for capsules, allowing for the simultaneous evaluation of multiple responses. All analyses were performed with three independent replicates (n=3), and results are presented as mean ± standard deviation. For the CCD, each experimental run was prepared and analyzed independently in triplicate. While certain biological responses exhibited R^2 values below 0.70, this is attributed to the inherent variability associated with microbial survival under multi-stress conditions. The statistical validity of the models was confirmed by significant p-values and non-significant Lack-of-Fit results. Furthermore, predictive accuracy was rigorously tested through a validation experiment under the calculated optimal conditions. To complement p-values and evaluate the practical magnitude of each factor, standardized regression coefficients (coded factors; Supplementary File 2) and percentage contributions to total model variation were used as effect-size metrics. Although family-wise corrections (e.g., Bonferroni) were not applied across multiple responses to avoid inflating Type II errors in quadratic response surface estimation, model validity and protection against Type I errors were confirmed through empirical triplicated validation at the multi-response optimum condition (Table 4).

Results and discussion

Encapsulated material characterization

Spray drying is the most critical stage determining the physical success of microencapsulation. The storage stability of the obtained encapsulated powders and the preservation of probiotics are directly related to the thermal changes during drying and the final moisture content of the product. The outlet temperature represents the actual temperature to which the particles in the drying chamber are exposed and plays a more decisive role in probiotic viability than the inlet temperature. It was observed that as the AYC concentration (B) in the matrix increased, the outlet temperature also increased, especially at high inlet air temperatures (Supplementary File 3) ($p < 0.0001$). This finding can be explained by changes in the heat transfer coefficients of feedstocks with high solid content. According to Lim et al. (2026), typical inlet and outlet temperatures in spray-drying studies range from 100 to 170 °C and 45 to 105 °C, respectively. Although lower outlet temperatures (optimally 85–90 °C) improve initial probiotic survival, they also increase moisture retention in the powders, thereby negatively affecting long-term viability. Shu et al. (2026) stated that the coating material concentration determines the encapsulation efficiency and that a high solid content increases protection but can make atomization difficult. According to the ANOVA results, the inlet temperature has the greatest effect on the outlet temperature ($p < 0.0001$). Each unit increase in the inlet air temperature linearly increased the outlet temperature. For example, at an inlet temperature of 150 °C, the outlet temperature reached 84 °C (Run 15), whereas at an inlet temperature of 120 °C, it dropped to 45 °C (Run 14). Pump speed (C) negatively affected the outlet temperature ($p = 0.0094$). Increasing the pump speed allowed more liquid to enter the drying chamber per unit time, thereby increasing evaporative cooling and decreasing the outlet temperature (Supplementary File 3). Shu et al. (2026) reported that the feed rate affects the dehydration time of probiotics and that an optimized feed rate prevents excessive drying. Dry matter analysis assesses the water-removal performance of the drying process and the powder's physical quality. In all runs, dry matter ratios ranged from 93.77% to 98.02% (Table 1). This indicates that the material adapts very well to spray drying and that the AYC does not inhibit water removal. Despite an R^2 of 0.4361, the model demonstrates a low $RMSE = 0.97\%$ and a $CV = 1.01\%$, with non-significant Lack-of-Fit ($p = 0.5826$) and Adequate Precision > 4.0 (5.58). This confirms that the model's absolute deviation is within the practical laboratory error range. The ANOVA results show that the pump speed (C) has a significant effect ($p < 0.05$) on the dry matter content (Table 2). The low pump speed resulted in forming drier particles by increasing the droplets' residence time in the drying chamber (Supplementary File 3). This is supported by the concurrent increase in the outlet temperature. Water activity must be below 0.3 throughout the shelf life of the powdered product to keep probiotics in a metabolic dormant state and prevent oxidative reactions. In this study, water activity values ranged from 0.098 to 0.335. The fact that the water activity values of most samples remained below 0.300 indicates that the drying process produced extremely stable powders from a microbiological perspective (Li et al., 2023). The developed mathematical model for water activity (a_w) demonstrated adequate predictive capability, characterized by a coefficient of determination (R^2) of 0.6254 and a low root mean square error ($RMSE = 0.043$). The model's suitability was further corroborated by a non-significant Lack-of-Fit test ($p = 0.2808$), confirming that the residual variation was primarily attributable to random experimental error rather than systematic model inadequacy. Moreover, the Adequate Precision value reached 7.76, substantially exceeding the minimum benchmark of 4.0, indicating an adequate signal-to-noise ratio and confirming that this model can reliably navigate the design space for process optimization. A decrease in the air inlet temperature and an increase in pump speed led to higher water activity (Supplementary File 3). The concentration (B) parameter showed

Table 1 Physicochemical properties of encapsulated powders and survival rates of *L.acidophilus* compared to free cells after drying. in vitro digestion. and during storage periods

Run	SD Outlet temperature (°C)	Water activity	Dry matter content (%)	*L.acidophilus* count (Pre Drying) (log CFU /mL)	*L.acidophilus* count (Post Drying) (log CFU /mL)	Survival rate *(%)*	*L.acidophilus* count (After gastric digestion) (log CFU / mL)	*L.acidophilus* count (After intestinal digestion) (log CFU / mL)	*L.acidophilus* count (After one month of storage) (log CFU / mL)	*L.acidophilus* count (After two months of storage) (log CFU /mL)	*L.acidophilus* (After three months of storage) (log CFU /mL)
Free cell	-	-	-	9.30±0.06	< 1.00 BDL*		1.22±0.07	0.52±0.03	-	-	-
1	82	0.125±0.009	97.79±0.12	9.28±0.06	7.50±0.28	80.65±0.09	6.56±0.08	5.49±0.12	7.3±0.01	6.07±0.26	5.75±0.16
2	61	0.178±0.002	96.57±0.17	9.32±0.07	7.64±0.05	82.15±0.18	6.65±0.09	5.42±0.04	6.90±0.35	6.21±0.07	5.89±0.29
3	58	0.256±0.003	95.52±0.06	9.31±0.05	7.27±0.38	78.17±0.36	6.11±0.36	4.91±0.13	6.68±0.03	5.65±0.08	5.21±0.06
4	76	0.098±0.002	98.02±0.02	9.29±0.08	7.17±0.18	77.10±0.12	6.08±0.31	4.99±0.16	6.30±0.04	5.08±0.20	4.88±0.10
5	72	0.141±0.012	97.90±0.11	9.30±0.06	6.98±0.03	75.05±0.11	5.85±0.29	5.04±0.23	6.27±0.05	5.37±0.29	4.81±0.16
6	65	0.177±0.018	97.44±0.09	9.33±0.05	7.60±0.43	81.72±0.48	6.39±0.20	5.46±0.62	6.88±0.24	5.93±0.38	5.82±0.57
7	68	0.217±0.021	96.50±0.03	9.27±0.07	7.18±0.10	77.20±0.09	5.47±0.02	4.68±0.18	6.28±0.01	5.30±0.26	5.18±0.04
8	61	0.148±0.006	97.78±0.07	9.31±0.06	7.17±0.18	77.10±0.18	5.93±0.41	5.71±2.14	6.88±0.05	5.57±0.26	5.38±0.16
9	56	0.244±0.009	96.05±0.11	9.28±0.05	6.46±0.25	69.46±0.03	4.98±0.01	4.05±0.39	5.46±0.28	4.43±0.44	4.31±0.18
10	62	0.201±0.003	95.86±0.13	9.30±0.07	7.60±0.17	81.72±0.18	6.47±0.04	5.88±0.07	7.03±0.06	6.29±0.70	6.15±0.82
11	71	0.230±0.007	95.52±0.15	9.32±0.06	6.33±0.11	68.06±0.03	5.68±0.09	5.28±0.01	6.08±0.09	5.40±0.06	5.13±0.15
12	65	0.228±0.011	95.49±0.21	9.29±0.05	6.50±0.37	69.89±0.03	5.77±0.04	5.31±0.16	6.38±0.25	5.14±0.17	4.79±0.07
13	61	0.281±0.015	95.74±0.12	9.31±0.08	7.18±0.10	77.20±0.05	6.37±0.19	5.62±0.03	6.72±0.09	5.85±0.15	5.31±0.15
14	45	0.335±0.022	93.77±0.33	9.30±0.06	7.50±0.23	80.65±0.18	5.80±0.04	5.29±0.08	7.25±0.24	6.20±0.49	5.88±0.23
15	84	0.134±0.003	96.51±0.16	9.29±0.07	5.53±0.07	59.46±0.01	4.20±0.13	3.76±0.31	5.45±0.04	4.69±0.22	4.14±0.20
16	82	0.149±0.009	96.62±0.07	9.30±0.05	6.76±0.55	72.69±0.05	5.61±0.1	4.89±0.12	6.69±0.12	5.27±0.08	4.85±0.07

Values are presented as mean ± standard deviation (n=3). *SD* spray dryer. Free cell viability indicates the high sensitivity of unencapsulated bacteria to simulated gastrointestinal conditions. BDL: Below detection limit ($< 1.0 logCFU/mL$), indicating complete cell mortality during spray drying without wall material; ‡ Powder storage was not applicable due to the complete absence of viable cells post-drying; gastrointestinal digestion of free cells was evaluated using fresh, non-dried cell suspensions. "N_0 corresponds to the viable cell concentration in the atomization feed prior to spray drying. Survival rate$(\%) = \left(logN/logN_0\right) \times 100$")

Table 2 Effects of process parameters on the physicochemical properties of encapsulated powders and survival rates of *L. acidophilus* after drying and in vitro digestion

Factor	Outlet temperature (°C)		Water activity		Dry matter content (%)		L.acidophilus count (Post Drying) (log CFU /mL)		L.acidophilus count (After gastric digestion) (log CFU /mL)		L.acidophilus count (After intestinal digestion) (log CFU /mL)		Survival rate (%)	
	SS	P value	SS	P value	SS	P value	SS	P value	SS	P value	SS	P value	SS	P value
Model	Linear (p=0.0001)		Linear (p=0.0067)		Linear (p=0.0067)		Linear (p=0.0032)		Modified Quadratic (p=0.0062)		Linear (p=0.0159)		Linear (p=0.0036)	
A-Inlet Temperature	1585.58	< 0.0001	0.018	0.4723	2.59	0.1231	0.8946	0.0257	0.0731	0.4574	0.0408	0.7172	103.65	0.0252
B-AYC Concentration	598.65	< 0.0001	0.0004	0.05	0.5189	0.4723	2.69	0.0008	2.65	0.0012	3.61	0.0045	311.57	0.0008
C-Pump Rate	81.67	0.0094	0.016	0.1231	4.47	0.05	0.0291	0.6544	0.0344	0.607	1.3	0.0586	3.40	0.6514
AC									0.8338	0.0277				
BC									0.4674	0.0812				
C2									1.1	0.0146				
Lack of fit	102.86		0.0229	0.2808	10.62	0.5826	1.38	0.831	0.642	0.9545	3.38	0.5413	1.91	0.8334
Pure Error	0		0.0003		0.6856		0.2729		0.4496		0.1812		31.66	
R2	0.9391		0.6254		0.4361		0.6707		0.8172		0.5642		0.6724	
Adj R2	0.9239		0.5317		0.2951		0.5883		0.6954		0.4552		0.5905	
Predicted R2	0.8991		0.3587		-0.1602		0.3265		0.2605		0.1722		0.3306	
RMSE	2.93		0.04		0.97		0.37		0.35		0.54		0.48	
C.V. %	4.38		22.38		1.01		5.29		6.48		11.49		5.27	
Adequate Precision	26.02		7.76		5.58		9.03		9.76		7.24		9.07	

Inlet air temperature (°C); B: AYC (autolyzed yeast cell) concentration (%, w/v); C: Feed pump rate (mL/min). AC and BC represent two-factor interaction terms, and C^2 represents the quadratic term. *SS* sum of squares, R^2: coefficient of determination, Adj R^2: adjusted R^2 Predicted R^2: predicted coefficient of determination, *RMSE* root mean square error; C.V. % coefficient of variation, Adequate Precision signal-to-noise ratio. Statistical significance was defined at $p < 0.05$. Non-significant lack-of-fit ($p > 0.05$) indicates adequate model validity and suitability for navigating the experimental design space

a statistically significant effect on water activity ($p < 0.05$). The increase in the amount of coating material affected the water-retention mechanism within the particles, thereby influencing the aw of the final product. The lowest water activity (0.098) was obtained at a high inlet temperature (150 °C) and a medium wall material concentration (20%). Combinations of high inlet temperature and low pump speed (such as Runs 4 and 15) have been found to be more effective in achieving the low water activity and high dry matter targets critical for the stability of powdered products. However, the stress effect of outlet temperatures above 80 °C on probiotic viability should also be considered.

Viability values and survival rates of encapsulated probiotic powders after drying

Spray drying exposes probiotic bacteria to harsh conditions, including high temperatures, dehydration, and osmotic stress. When unencapsulated (free) *L. acidophilus* was subjected to the spray drying process without carrier materials, viable cell recovery was completely compromised, falling below the analytical detection limit ($< 1.0 log CFU/mL$, Table 1). This confirmed that unprotected *L. acidophilus* cannot survive the rapid thermal dehydration of the drying chamber on its own. Using AYC, viability values after the drying process ranged from 5.53 to 7.64 log CFU/mL (Table 1). According to the ANOVA results (Table 2), the coating concentration had the greatest effect on viability ($p = 0.0008$). When the wall material concentration increased from 10 to 20%, viability was generally maintained, but a dramatic decrease was observed at 30% (Run 15). The inlet temperature also significantly affected viability ($p = 0.0257$). In particular, at high inlet temperatures and low feed rates (Run 15), the outlet air temperature rose to 84 °C, crossing a critical thermal threshold at which heat-induced macromolecular denaturation overwhelms the physical insulation of the yeast cell wall. Although the direct effect of pump speed on post-drying viability was not statistically significant ($p = 0.6544$), this parameter remains an essential operational control in spray-drying. Within the experimental model, its influence is primarily reflected in its contribution to the overall stability of the outlet temperature, a critical determinant of cell survival. Therefore, although pump speed did not independently affect the final counts, it is necessary to optimize it to maintain the desired thermal conditions within the drying chamber (Supplementary File 4). Palamutoğlu & Sarıçoban (2013) stated that the solution concentration of the material used to form the capsule and the final particle size are the most important factors for survival rates. The highest viability and survival rate in Run 2 (135 °C inlet, 10% concentration, 10 mL/min pump speed) were 7.64 log CFU/mL and 82.15%, respectively. This indicates that moderate temperature and low solids content enable cells to overcome the instantaneous dehydration shock more easily. The lowest viability and survival rate were measured in Run 15 (5.53 log CFU/mL and 59.46%). In this run, the combination of a high inlet temperature (150 °C), a high concentration (30%), and a low pump rate (6 mL/min) subjected the cells to excessive thermal stress, revealing that the coating matrix could not provide sufficient protection at this temperature. The β-glucan and mannoproteins in the yeast cell biomass form a shield around the cell during drying, limiting direct heat contact and oxygen transfer. The high viability rates (especially at 7 log levels) indicate that the porous structure of the yeast cell wall allows moisture transfer while protecting vital cellular components. For the encapsulation of *L. acidophilus* cells, low and medium temperatures (120–135 °C) and a low-medium wall material concentration (10–20%) appear ideal for maximum survival. Concentration levels of 30% may increase viscosity, making atomization more difficult and prolonging drying time, potentially exposing the cells to heat for a longer period. Additionally, methodological constraints associated with standard pour-plate counting on MRS agar must be recognized. Rapid atomization and moisture flash-off can induce a viable but non-culturable (VBNC) state, wherein injured cells maintain intact membranes and metabolic potential but fail to replicate on solid media. Although pre-plating rehydration in phosphate buffer served as a resuscitation step, plate counts likely represent a conservative estimate of surviving cells. Future research should leverage culture-independent analytical techniques, such as flow cytometry with SYTO 9/propidium iodide (LIVE/DEAD) dual-staining or propidium monoazide (PMA)-qPCR, to quantitatively delineate the true viable, dead, and VBNC cell fractions.

Viability values after in vitro digestion

To exert their health-promoting effects, probiotics must survive harsh biological barriers, such as gastric acidity and bile salts, to reach the colon in sufficient numbers. In this study, the protective efficacy of AYC as a shield for *L. acidophilus* was evaluated using a simulated in vitro gastrointestinal (GI) transit model. Freshly prepared free bacterial suspensions ($9.30 \pm 0.08 log CFU/mL$) were subjected directly to in vitro digestion alongside the spray-dried AYC microcapsules. Free cells exhibited severe sensitivity: exposure to simulated gastric juice triggered a dramatic decline from $9.30 \pm 0.06 log CFU/mL$ to $1.22 \pm 0.07 log CFU/mL$, which further dropped $0.52 \pm 0.03 log CFU/mL$ following exposure to intestinal fluid and bile salts. This near-total mortality demonstrates that naked probiotics fall far below the $6.0 log CFU/mL$ therapeutic threshold within the upper digestive tract. During the gastric phase, the viability of *L. acidophilus* across different treatments ranged from 4.20 to 6.65 log CFU/mL (Table 1). The highest resistance was observed

in Run 2 (6.65 log CFU/ mL) and Run 10 (6.47 log CFU/ mL), whereas Run 15 exhibited the lowest survival. Wall material concentration (B) had a highly significant impact on gastric viability ($p = 0.0012$) (Table 2). Furthermore, the quadratic effect of pump speed (C^2, $p = 0.0146$) and the interaction between inlet temperature and pump speed (AC, $p = 0.0277$) were critical determinants of survival. While higher matrix concentrations generally improved protection, samples exposed to excessive thermal stress during drying lost physical integrity more rapidly when exposed to acids. These findings align with previous studies demonstrating the vulnerability of free cells. For instance, Fávaro-Trindade & Grosso (2002) reported that free *L. acidophilus* cells were eliminated within 1 h. at pH 1.0, whereas encapsulated forms remained above the therapeutic threshold (6–7 log CFU/mL). Similarly, it was observed that free cells of Lactobacillus species were destroyed almost immediately, within 60 min of gastric exposure, while AYC and β-glucan matrices maintained measurable viability (Ismail et al., 2025; Shah et al., 2016). This protection was attributed to the especially 100–200 nm-thick yeast cell wall, which acts as a physical barrier, minimizing the diffusion of gastric juice into the capsule core (Han et al., 2016). Upon transitioning to the intestinal phase, viability values further declined to 3.76–5.88 log CFU/mL. For the biological response of intestinal viability, the model yielded an R^2 value of 0.5642, which, while moderate, is consistent with the inherent physiological variability encountered in live bacterial enumeration following sequential acid and bile exposure. The model exhibited acceptable precision with an RMSE of 0.54 log CFU/mL and a coefficient of variation (*CV*) of 11.49%. Importantly, the model's validity was underpinned by a statistically non-significant Lack-of-Fit ($p = 0.5413$) and an Adequate Precision ratio of 7.24 (> 4.0), demonstrating that the regression model provides a reliable empirical approximation for exploring multi-stress survival during in vitro digestion. Run 10 emerged as the most successful combination (120 °C inlet temperature, 20% concentration), yielding a final intestinal viability of 5.88 log CFU/mL. In the intestinal phase, coating concentration remained the dominant parameter ($p = 0.0045$). Although the pump rate was not statistically significant at the conventional threshold ($p = 0.0586$), it showed a trend toward significance, suggesting a minor practical effect on particle residence time. This suggests that the feed delivery rate may play a marginal role in the protective capacity of the resulting powder, likely by influencing the overall exposure time to heat during particle formation. The observed 0.5–1.0 log reduction during the transition from gastric to intestinal conditions is likely due to the increased sensitivity of acid-stressed cells to the detergent-like effects of bile salts. While previous literature noted that pure alginate microcapsules frequently disintegrate at the neutral pH of the simulated intestine, leading to burst release (Ahmadi et al. 2025), the AYC matrix maintained stable, viable populations throughout intestinal transit (up to 5.88 log CFU/mL in Run 10). It is hypothesized that the carbohydrate-protein matrix characteristic of yeast cell walls, evidenced by the persistent FTIR polysaccharide absorption bands at 1028 and 520 cm^{-1} and enhanced β-sheet protein structures, may delay digestive fluid diffusion and mitigate bile-salt solubilization. Nevertheless, because parallel control runs using conventional wall materials (such as pure sodium alginate or maltodextrin) were not performed in this study, direct claims of superiority cannot be made, and comparative benefits remain prospective hypotheses to be validated through head-to-head empirical trials.

The robustness of the AYC-based system is attributed to the unique biophysical properties of β-glucan and mannoproteins. These components create a structurally resistant matrix that delays the penetration of digestive fluids (Gani et al., 2018; Mokhtari et al., 2017). Furthermore, the co-aggregation between *L. acidophilus* and the yeast cell surface may create a synergistic biofilm that enhances metabolic resistance (Han et al., 2016). In conclusion, the integration of autolyzed yeast cell walls provides a multifaceted protective mechanism, acting as a physical shield against acid, a barrier against bile-induced lysis, and a potential prebiotic substrate, thereby ensuring the effective delivery of *L. acidophilus* to the lower gastrointestinal tract.

Viability values after storage

One of the primary objectives of microencapsulation is to prevent the loss of probiotic viability during storage at room temperature or refrigerated conditions (4 °C) by maintaining the cells in a dormant state. AYC contributes significantly to this stability by acting as a barrier to the permeation of moisture and oxygen. In the present study, viability levels after 90 days of storage at 4 °C ranged from 4.14 to 6.15 log CFU/mL (Table 1). The formulations from Runs 10 (6.15 log CFU/mL) and 14 (5.88 log CFU/mL) were the most stable. Notably, the high viability maintained by Run 10 suggests that a lower inlet temperature (120 °C) preserves the long-term robustness of the cells. Conversely, Run 15 exhibited the lowest viability (4.14 log CFU/mL), indicating that high thermal stress during drying (outlet temperature of 84 °C) exhausts cellular repair mechanisms, leaving the probiotics more vulnerable to storage-related stress. The long-term viability model after one month of refrigerated storage exhibited strong statistical reliability, exhibiting a low error index ($RMSE = 0.34 log CFU/mL$) and excellent experimental repeatability with a *CV* of only 5.28%. The model displayed an Adequate Precision value of 7.92, indicating an ample discrimination signal relative to background noise. Furthermore, the non-significant Lack-of-Fit ($p = 0.7709$) confirmed that the linear formulation captured the primary

preservation trends without significant model bias, validating its utility for predicting shelf-life stability. Statistical analysis revealed that coating concentration was the most dominant factor affecting stability throughout the first (p = 0.0003), second (p = 0.0037), and third (p = 0.0022) months of storage (Table 3). While the inlet temperature was not statistically significant in the early stages, it became statistically significant by the third month (p = 0.0268), indicating that heat-induced damage becomes more pronounced over time (Supplementary File 5). Ismail et al. (2025) reported that *L. brevis* C23 encapsulated with *S. cerevisiae* cell walls showed significantly higher stability at 4 °C compared to sodium alginate and free cells. While free cells faced devastating losses (dropping from 7.84 to 0.20 log CFU/mL), the AYC-encapsulated cells maintained a robust profile, losing only 1.19 log CFU/mL over 8 weeks. Ahmadi et al. (2025) utilized Arrhenius kinetic modeling to show that AYC and β-glucan formulations maintained viability above the critical 6 log CFU/mL threshold for 56 days at various temperatures, whereas pure alginate capsules failed completely. β-glucan acts as a dual-purpose material, acting as both a physical shield and a prebiotic substrate. It was observed that β-glucan matrices effectively protected Lactobacillus species from environmental stressors that caused total mortality in free cell populations within 60 days (Gani et al., 2018; Shah et al., 2016). The results indicate that to maintain *L. acidophilus* above the safety and therapeutic limit of 6 log CFU/mL for 90 days, the conditions of Run 10 (120 °C inlet, 20% concentration) are optimal. The yeast cell wall's glucan, mannan, and chitin composition provides structural integrity, effectively shielding probiotics from the oxidative and moisture-related challenges of their surroundings. This results in a longer shelf life than traditional wall materials.

Determination of the optimum conditions

To identify the most effective spray-drying parameters, a multi-response desirability function analysis was performed, and to verify the validity of the mathematical models, a validation study was conducted to compare predicted response values with experimental results. The numerical optimization aimed to maximize the viability of *L. acidophilus* throughout all stages: post-drying, gastrointestinal transit, and long-term storage, while also maintaining a high dry matter content and low water activity (aw). The desirability function assigns a score from 0 to 1 to each response, where 1 represents the ideal target. The individual desirability scores are then combined into a single global desirability (D) value. The model identified the following optimized conditions: an inlet air temperature of 145.6 °C, a wall material concentration of 10%, and a feed pump rate of 8.95 mL/min, resulting in an overall desirability score of 0.783. Under these specific conditions, the model predicted an intestinal viability of 5.18 log CFU/ mL and a 3-month storage stability of 5.45 log CFU/mL. When these conditions were tested experimentally, the observed values showed a high degree of correlation with the predicted data, with deviations remaining within the 5% error margin. For

Table 3 Effects of process parameters on the viability of *L.acidophilus* during storage periods

Faktör	Survival rates after one month of storage (log CFU /mL)		Survival rates after two months of storage (log CFU/mL)		Survival rates after three months of storage (log CFU mL)	
	SS	P value	SS	P value	SS	P value
Model	Linear (p=0.0024)		Linear (p=0.0195)		Linear (p=0.0067)	
A-Inlet Temperature	0.0705	0.456	0.426	0.1498	0.962	0.0268
B-AYC Concentration	3.08	0.0003	2.33	0.0037	2.27	0.0022
C-Pump Rate	0.0496	0.5306	3.36E−06	0.9966	0.0252	0.6901
Lack of fit	1.24	0.7709	1.83	0.8108	1.41	0.8972
Pure Error	0.1833		0.3264		0.4053	
R^2	0.6851		0.5481		0.6253	
Adj R^2	0.6063		0.4351		0.5316	
Predicted R^2	0.3566		0.1486		0.3107	
RMSE	0.34		0.42		0.39	
C.V. %	5.28		7.69		7.44	
Adequate Precision	7.92		6.26		8.29	

Inlet air temperature (°C); B AYC (autolyzed yeast cell) concentration (%, w/v); C: Feed pump rate (mL/min). AC and BC represent two-factor interaction terms, and C^2 represents the quadratic term. *SS* sum of squares; R^2 coefficient of determination; Adj R^2: adjusted R^2, Predicted, R^2: Predicted coefficient of determination, *RMSE* Root mean square error, C.V. % coefficient of variation, Adequate Precision: Signal-to-noise ratio. Statistical significance was defined at $p < 0.05$. Non-significant lack-of-fit ($p > 0.05$) indicates adequate model validity and suitability for navigating the experimental design space

instance, the experimental intestinal survival was 5.25 ± 0.12 log CFU/mL, which closely matched the theoretical prediction (Table 4). This strong alignment confirms that the Response Surface Methodology (RSM) effectively captured the complex interactions between the spray-drying parameters and the protective capacity of the autolyzed yeast cell wall matrix. Consequently, these findings validate the autolyzed yeast cell wall as a robust and predictable encapsulating agent for stabilizing sensitive probiotics in functional food applications. The operational trade-offs inherent in the experimental design must also be acknowledged. The 3-factor, 3-level Face-Centered Central Composite Design was adopted to avoid infeasible operational combinations that lead to atomization failures and chamber wall deposition in laboratory-scale spray drying. While the multi-response desirability function effectively converged on a viable operational sweet spot, corroborated by validation runs with experimental values falling strictly within the computed 95% Confidence Intervals, future scale-up studies should employ expanded designs with larger run sets to more fully resolve subtle multi-factor quadratic curvatures.

SEM images

The morphological attributes of microcapsules provide immediate insight into the heat transfer mechanisms and particle-formation processes inherent to spray-drying. Examination of SEM micrographs in this investigation revealed clear distinctions between the control group and the optimized formulations, underscoring the enhanced film-forming capacity of AYC. The control group (Fig. 1) showed irregular particle sizes and a prevalence of large, agglomerated structures. The particles' rough, porous surfaces likely resulted from the high surface tension induced by rapid moisture evaporation during drying. The clustering of smaller particles around larger ones in the control samples suggests poor flowability and potentially hindered solubility in food applications. Conversely, microcapsules synthesized under optimum conditions exhibited considerably greater uniformity and were predominantly spherical. These particles possessed a continuous, undamaged surface, demonstrating high structural integrity. Such smooth surfaces are essential indicators of stability, as they reduce the core probiotic material's exposure to external degrading elements, including oxygen, moisture, and light. Moreover, the lack of cracks and fissures accounts for the improved survival of *L. acidophilus* during simulated gastrointestinal transit, the intact wall impedes the penetration of gastric acids. According to Ismail et al. (2025), AYC wall-based capsules are generally smaller (approx. 51–54 µm) and more uniform compared to the larger, bulkier structures formed by sodium alginate (approx. 80–84 µm). This is attributed to the β-glucan polymers within the yeast wall, which create a dense, intertwined fibrous cage that effectively entraps the probiotic cells. Reyes et al. (2018) observed that maltodextrin and gum arabic often result in shriveled or dented surfaces due to rapid evaporation; the AYC matrix maintains a more robust spherical shape. The balloon-like clusters observed in our study and reported by Sultana et al. (2017) are a hallmark of β-glucan-binding properties. Studies characterize the internal structure of β-glucan matrices as honeycomb-like, with pore sizes ranging from 14.2 to

Table 4 Predicted versus experimental results at the optimum points

Response parameter	Predicted value	Experimental value (Mean ± SD)	Relative error (%)
Physical properties			
SD outlet temperature (°C)	70.81	71.25 ± 0.85	0.62
Water activity (aw)	0.157	0.161 ± 0.004	2.56
Dry matter content (%)	97.10	96.85 ± 0.42	0.25
L.acidophilus Viability (log CFU/mL)			
Initial count (Post-Drying)	7.30	7.24 ± 0.11	0.82
After gastric digestion	6.14	6.08 ± 0.15	0.97
After intestinal digestion	5.18	5.25 ± 0.12	1.35
L.acidophilus Storage Stability (log CFU/mL)			
Month 1 (4 °C)	6.97	6.89 ± 0.09	1.14
Month 2 (4 °C)	5.83	5.76 ± 0.14	1.20
Month 3 (4 °C)	5.45	5.51 ± 0.18	1.10
Overall desirability	**0.783**	–	–

Values for experimental results are expressed as mean ± standard deviation (n=3). Relative error was calculated as (Predicted—Experimental) / Predicted × 100. SD: Spray dryer

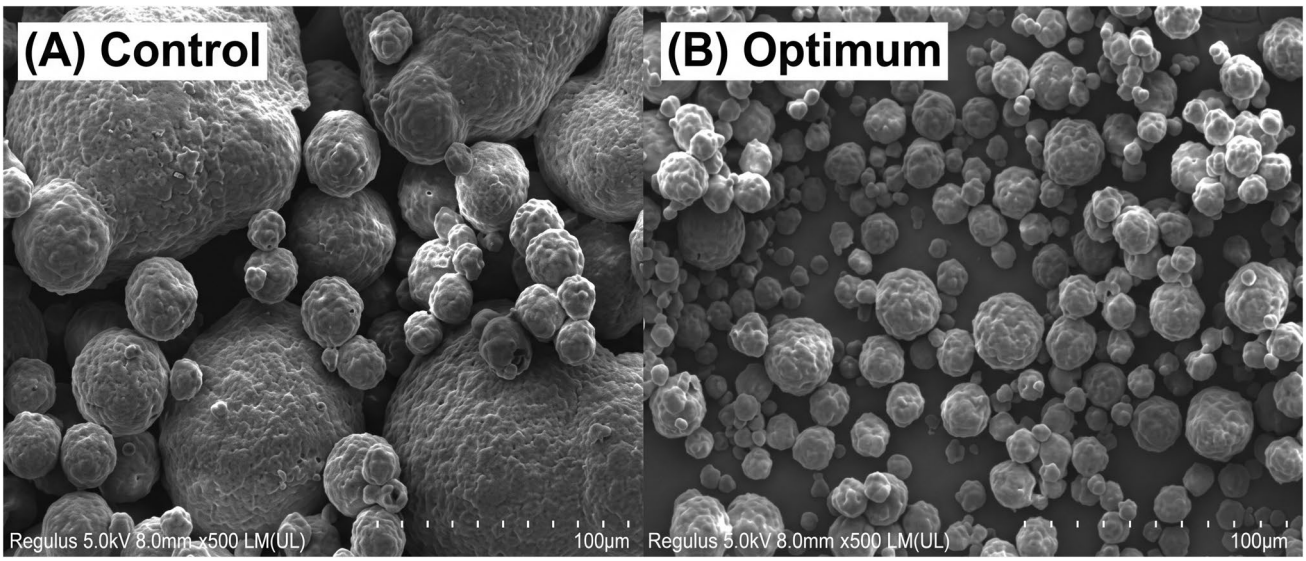

Fig.1 Scanning electron micrographs (SEM) illustrating particle morphology. (A) Control group (unencapsulated, spray-dried autolyzed yeast cell biomass) showing irregular shapes, surface pores, and aggregate clustering (500×, scale bar = $100\mu m$). (B) Optimized microcapsules (inlet temperature $145.6°C$, AYC concentration 10%, pump rate $8.95mL/min$) exhibiting continuous, smooth, spherical shells without cracks or deep indentations (500×, scale bar = $100\mu m$)

16.3 µm (Gani et al., 2018; Shah et al., 2016). This multifaceted structure provides superior mechanical strength against processing stresses while facilitating a controlled release of the probiotics in the target intestinal environment. The transition from a porous, irregular morphology in the control samples to a dense, smooth, and spherical structure in the optimized AYC microcapsules confirms that this novel wall material acts as a superior encapsulating agent. This structural robustness is the primary factor driving the high viability and long-term stability of *L. acidophilus* observed in this research. While SEM analysis provides valuable insight into the surface integrity and spherical shape of the microcapsules, it primarily depicts external surface features. The absence of noticeable cracks and fissures suggests a coherent wall structure that physically limits the rapid diffusion of acidic gastric juices and oxygen into the core. However, conclusive confirmation of protective efficacy and delayed release is derived from viability retention profiles during in vitro simulated gastrointestinal transit, in which encapsulated cells exhibited significantly higher survival than free cells.

FTIR spectra

Fourier Transform Infrared Spectroscopy (FTIR) was used to investigate chemical interactions and conformational changes within the microencapsulation matrix. The 3268 cm^{-1} region corresponds to N–H stretching vibrations in proteins and to O–H stretching associated with water or hydrogen bonding (Fig. 2). The enhanced intensity of this peak in the optimized sample indicates stronger hydrogen bonding, which, in turn, contributes to a more durable, stable matrix. The 2920 cm^{-1} band is associated with aliphatic C-H bonds, and the lack of significant shifting in this band indicates that the primary carbon skeleton of the wall material remained intact during the process. The 1624 cm^{-1} band is the most critical region for protein secondary structure, and this peak primarily represents C=O stretching. The higher intensity observed in the optimized sample compared to the control correlates directly with an increase in β-sheet structures (typically found in the 1620–1640 cm^{-1} range). The 1527 cm^{-1} band corresponds to N–H bending and C-N stretching. The sharpening of this peak in the optimized sample further indicates a more organized protein conformation. The 1028 cm^{-1} and 520 cm^{-1} bands are indicative of carbohydrate groups (C-O and C–C stretching) present in the AYC polysaccharides. The heightened intensity in these regions implies more robust molecular interactions among the wall material constituents. A notable alteration in the secondary structure was a considerable increase in β-sheet content, accompanied by a reduction in α-helix and random coil structures. A higher amount of β-sheet is associated with greater thermal stability and a stronger physical barrier. This is crucial for protecting the probiotics inside from oxidative stress and moisture. This transition suggests the formation of a tighter, denser, and more resistant protein network, which is essential for protecting the encapsulated probiotics from oxidative stress and moisture. A decrease in random coil structures suggests a transition of the protein matrix from a disordered, flexible state to a more structured and compact

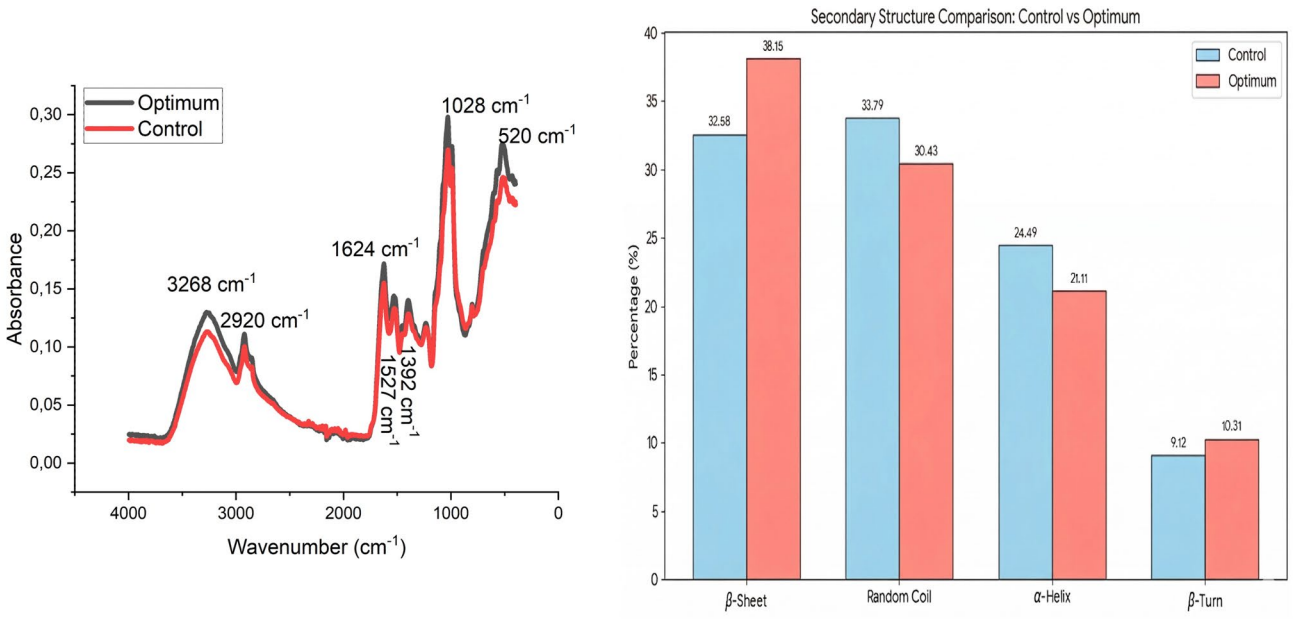

Fig.2 FTIR spectra and secondary protein conformation analysis. (A) Comparative infrared absorbance spectra of control AYC biomass and optimized microcapsules between 4000 and 500 cm^{-1} with functional group assignments: 3268 cm^{-1} (N–H/O–Hstretching; Amide A / hydrogen bonding), 2920 cm^{-1} (aliphatic C–H stretching), 1624 cm^{-1} (C=O stretching / β-sheet secondary structure; Amide I), 1527 cm^{-1} (N–H bend / C–N stretch; Amide II), and 1028 cm^{-1}/ 520 cm^{-1} (C–O/C–Cring vibrations of β-glucan and mannoproteins). (B) Deconvoluted secondary structure percentage distributions (Amide I band, 1600–1700 cm^{-1})comparing control vs. optimized microcapsules

form. This structural change reduces the matrix's porosity, thereby inhibiting the early release of the core substance and enhancing its controlled-release properties. Consequently, the resulting wall material exhibits increased resistance to both mechanical and thermal stress, while also functioning as a more effective impermeable barrier, thereby facilitating the successful delivery of *L. acidophilus* to its intended destination.

Heat stability

Thermal resilience is a critical prerequisite for incorporating probiotic microcapsules into processed functional foods. Quantitative evaluation of thermal inactivation kinetics revealed that the autolyzed yeast cell wall provides notable heat insulation compared to unprotected free cells. Prior to thermal processing, the spray-dried microcapsules from the optimized run exhibited an initial viable count of $7.24 \pm 0.11 logCFU/mL$. At 65 °C, the AYC matrix conferred robust physical protection: viable counts remained virtually unchanged during the first two minutes ($6.186 \pm 0.015 logCFU/mL$ at 1 min and $6.190 \pm 0.020 logCFU/mL$ at 2 min), before declining slightly to $5.695 \pm 0.330 logCFU/mL$ after 3 min (Supplementary File 6). This reflects an overall log reduction of only $1.55 log$ units, allowing the surviving population to remain near the recommended therapeutic threshold of $10^6 CFU/mL$. In stark contrast, unprotected free cells suffered rapid thermal death at 65 °C, plummeting by $4.45 log$ units within 1 min ($4.85 \pm 0.18 logCFU/mL$) and dropping below the analytical detection limit ($< 1.00 logCFU/mL$) after 3 min. We hypothesize that this heat-buffering capacity is related to the low thermal diffusivity of the densely packed yeast wall macromolecular network, although direct compositional fractionation and comparative trials with conventional encapsulants will be required to confirm this mechanism. A definitive thermal threshold was identified at 75 °C. While encapsulated cells demonstrated partial survival during initial transient heating ($3.284 \pm 0.120 logCFU/mL$ at 1 min), extending exposure to 2 and 3 min resulted in complete loss of culturable viability ($< 1.00 logCFU/mL$). At 85 °C, rapid thermal denaturation of cellular components overwhelmed matrix protection, leaving only residual survival at 1 min ($1.778 \pm 0.010 logCFU/mL$) and complete inactivation thereafter. Free cells showed no survival ($< 1.00 logCFU/mL$) at any tested interval at 75 °C or 85 °C. The heat-buffering capacity of the AYC matrix at $\leq 65°C$ is primarily attributable to the low thermal diffusivity of the densely packed β-glucan and mannoprotein polymers. As demonstrated by FTIR deconvolution, the microencapsulation process promoted an increase in rigid β-sheet conformations (increasing from 32.58% in the control to 38.15%

in the optimum, Fig. 2), establishing an intermolecular hydrogen-bonded network that delays convective and conductive heat transfer to the enclosed bacterial core. Ismail et al. (2025) found that while free probiotic cells usually lose viability at temperatures around 50 °C, cells encapsulated within *S. cerevisiae* cell walls maintain viability up to 65 °C. The β-glucan matrix functions as a strong thermal insulation barrier, protecting the internal microbial components. Generally, heat treatment causes fatal damage to free cells by denaturing nucleic acids and proteins and breaking the bonds between their building blocks. In free cells, a 10-min exposure to 55 °C can decrease the count from 9.28 to 5.23 log CFU/mL. Conversely, AYC wall-encapsulated cells present a physical barrier that impedes the degradation of these essential molecular components (Shah et al., 2016). The polysaccharide composition, structure, and elevated molecular weight of β-glucan within the yeast cell wall establish a strong physical shield. This matrix effectively hinders direct heat transfer to the probiotic core, thus increasing the thermal tolerance of *L. acidophilus*. Consequently, these results confirm that AYC is a suitable wall material for probiotic delivery systems that may undergo moderate thermal processing in the food industry. These quantitative boundaries establish operational guidelines for industrial processing. The ability of AYC capsules to sustain $> 5.6 log CFU/mL$ across 3 min at 65 °C indicates that this delivery system is suitable for low-temperature batch processes (such as mild thermization at $60-65^{\circ}C$), warm beverage reconstitution (e.g., instant functional soups or warm teas), and direct incorporation into functional confectionery (such as gummies and jellies added during the cooling stage before gelatinization). However, because viability is lost at $\geq 75^{\circ}C$ within 2 min, unmodified AYC microcapsules are unsuitable for continuous High-Temperature Short-Time (HTST) pasteurization ($72^{\circ}C$ for 15 s) or baking applications. For products requiring processing temperatures above 75 °C, combining AYC with exogenous glass-forming disaccharides (e.g., trehalose) or applying enteric lipid/wax composite shells will be necessary to prevent ribosome denaturation and membrane collapse.

Supplementary Information The online version contains supplementary material available at https://doi.org/10.1007/s10068-026-02351-1.

Acknowledgements This study was supported by the Scientific Research Projects Coordination Unit of Eskisehir Osmangazi University (Eskisehir, Turkey) (ESOGU Project Number: FBA-2023-2829).

Author contributions Ilyas Atalar: Conceptualization, Methodology, Supervision, Writing – original draft. Sibel Yılmaz: Writing – original draft, Formal Analysis. Tahra El-Obeid: Writing – review & editing. Formal Analysis. Ömer Said Toker: Writing – review & editing. Şirin Oba İlter: Writing – review & editing, Formal Analysis. Abdullah Kurt: Writing – review & editing, Formal Analysis. Muhammet Irfan Aksu: Writing – review & editing. Nevzat Konar: Writing – review & editing. Conceptualization.

Funding This work was funded by Scientific Research Projects Coordination Unit of Eskisehir Osmangazi University, FBA-2023-2829, İlyas Atalar.

Data availability The data will be available from the corresponding author.

Declarations

Conflict of interest The authors declare no conflicts of interest or competing financial interests.

References

Ahmadi, M., Hashempour-baltork, F., Shojaee-Aliabadi, S., Marand, M. J., Shahraz, F., Mortazavian, A. M., & Hosseini, S. M. (2025). Effect of yeast cell wall and β-glucan on survival of Lactobacillus acidophilus LA-5 encapsulated in spray-dried cross-linked alginate microcapsules. *LWT*. https://api.semanticscholar.org/CorpusID:277143022

Amiri, S., Rezaei Mokarram, R., Sowti Khiabani, M., Rezazadeh Bari, M., & Alizadeh Khaledabad, M. (2019). Exopolysaccharides production by Lactobacillus acidophilus LA5 and Bifidobacterium animalis subsp. lactis BB12: Optimization of fermentation variables and characterization of structure and bioactivities. *International Journal of Biological Macromolecules*, *123*, 752–765. https://doi.org/10.1016/j.ijbiomac.2018.11.084

Borchani, C., Fonteyn, F., Jamin, G., Paquot, M., Thonart, P., & Blecker, C. (2016). Physical, functional and structural characterization of the cell wall fractions from baker's yeast Saccharomyces cerevisiae. *Food Chemistry*, *194*, 1149–1155. https://doi.org/10.1016/j.foodchem.2015.08.106

Brodkorb, A., Egger, L., Alminger, M., Alvito, P., Assunção, R., Ballance, S., Bohn, T., Bourlieu-Lacanal, C., Boutrou, R., Carrière, F., Clemente, A., Corredig, M., Dupont, D., Dufour, C., Edwards, C., Golding, M., Karakaya, S., Kirkhus, B., Le Feunteun, S., … Recio, I. (2019). INFOGEST static in vitro simulation of gastrointestinal food digestion. *Nature Protocols*, *14*(4), 991–1014. https://doi.org/10.1038/s41596-018-0119-1

ElObeid, T., Tüzün, B., Apaydın, A., Toker, O. S., Doguer, C., Palabiyik, I., Aksu, M. I., Konar, N., & Atalar, İ. (2025). Using autolyzed and dried Saccharomyces cerevisiae as various macromolecules and sucrose substitute: Developing novel gummy. *Food Chemistry: X*, *31*(February). https://doi.org/10.1016/j.fochx.2025.103045

Fávaro-Trindade, C. S., & Grosso, C. R. F. (2002). Microencapsulation of L. acidophilus (La-05) and B. lactis (Bb-12) and evaluation of their survival at the pH values of the stomach and in bile. *Journal of Microencapsulation*, *19*(4), 485–494. https://doi.org/10.1080/02652040210140715

Firdaus, T. R., Pranoto, Y., Brueck, W. M., & Witasari, L. D. (2025). Probiotic encapsulation using porous starch from arrowroot (Maranta arundinacea). *Food Chemistry Advances*, *8*(August), 101077. https://doi.org/10.1016/j.focha.2025.101077

Gani, A., Shah, A., Ahmad, M., Ashwar, B. A., & Masoodi, F. A. (2018). β-D-glucan as an enteric delivery vehicle for probiotics. *International Journal of Biological Macromolecules*, *106*, 864–869. https://doi.org/10.1016/j.ijbiomac.2017.08.093

Günal-Köroğlu, D., Bilgin, A. B., Karabulut, G., Saricaoglu, B., & Capanoglu, E. (2024). Encapsulation of hydrophobic compounds in yeast cells: methods, characterization, and applications. *Exploration of Foods and Foodomics*, *2*(3), 252–274. https://doi.org/10.37349/eff.2024.00037

Guo, Q., Li, S., Tang, J., Chang, S., Qiang, L., Du, G., Yue, T., & Yuan, Y. (2022). Microencapsulation of Lactobacillus plantarum by spray drying: Protective effects during simulated food processing, gastrointestinal conditions, and in kefir. *International Journal of Biological Macromolecules*, *194*(August 2021), 539–545. https://doi.org/10.1016/j.ijbiomac.2021.11.096

Han, L. N., Van, L. H. H., Duc, T. Van, & Dao, D. T. A. (2016). Encapsulation of Lactobacillus Acidophilus in Yeast Cell Walls (Saccharomyces Cerevisiae) for Improving Survival in Gastrointestinal Conditions. *Vietnam Journal of Science and Technology*, *54*(4), 533. https://doi.org/10.15625/0866-708x/54/4/7422

Ismail, A. S., Sreedharan, D. K., Ng, Z. J., & Tan, J. S. (2025). Microencapsulation of Lactobacillus cells utilizing the β-glucan-rich cell wall of Saccharomyces cerevisiae for enhanced stability and efficacy. *International Journal of Biological Macromolecules*, *311*. https://doi.org/10.1016/j.ijbiomac.2025.143971

Kayanna, N., Suppavorasatit, I., Bankeeree, W., Lotrakul, P., Punnapayak, H., & Prasongsuk, S. (2022). Production of prebiotic aubasidan-like β-glucan from Aureobasidium thailandense NRRL 58543 and its potential as a functional food additive in gummy jelly. *LWT*, *163*. https://doi.org/10.1016/j.lwt.2022.113617

Li, H., Peng, F., Lin, J. X., Xiong, T., & Huang, T. (2023). Preparation of probiotic microcapsules using gelatin-xylooligosaccharides conjugates by spray drying: Physicochemical properties, survival, digestion resistance and colonization. *Food Bioscience*, *52*(235), 102462. https://doi.org/10.1016/j.fbio.2023.102462

Lim, H. X. E., Choo, S. R., & Cheow, W. S. (2026). Chemical structures of encapsulants and their mechanisms of protection for spray-dried probiotics: a review. In *Applied Food Research* (Vol. 6, Number 1). Elsevier B.V. https://doi.org/10.1016/j.afres.2025.101580

Mokhtari, S., Jafari, S. M., Khomeiri, M., Maghsoudlou, Y., & Ghorbani, M. (2017). The cell wall compound of Saccharomyces cerevisiae as a novel wall material for encapsulation of probiotics. *Food Research International*, *96*, 19–26. https://doi.org/10.1016/j.foodres.2017.03.014

Ngoc Le, T. A., & Chen, W. N. (2025). Microencapsulation of Lactobacillus plantarum by avocado seed- type 3 resistant starch and okara protein isolate. *Food Chemistry Advances*, *7*(December 2024), 100964. https://doi.org/10.1016/j.focha.2025.100964

Palamutoğlu, R., & Sarıçoban, C. (2013). Microencapsulation of Probiotic Microorganisms. *Akademik Gıda*, (11(1)), 88–96. http://www.academicfoodjournal.com

Rajam, R., & Anandharamakrishnan, C. (2015). Spray freeze drying method for microencapsulation of Lactobacillus plantarum. *Journal of Food Engineering*, *166*, 95–103. https://doi.org/10.1016/j.jfoodeng.2015.05.029

Reyes, V., Chotiko, A., Chouljenko, A., & Sathivel, S. (2018). Viability of Lactobacillus acidophilus NRRL B-4495 encapsulated with high maize starch, maltodextrin, and gum arabic. *LWT*, *96*, 642–647. https://doi.org/10.1016/j.lwt.2018.06.017

Semyonov, D., Ramon, O., & Shimoni, E. (2011). Using ultrasonic vacuum spray dryer to produce highly viable dry probiotics. *LWT - Food Science and Technology*, *44*(9), 1844–1852. https://doi.org/10.1016/j.lwt.2011.03.021

Shah, A., Gani, A., Ahmad, M., Ashwar, B. A., & Masoodi, F. A. (2016). β-Glucan as an encapsulating agent: Effect on probiotic survival in simulated gastrointestinal tract. *International Journal of Biological Macromolecules*, *82*, 217–222. https://doi.org/10.1016/j.ijbiomac.2015.11.017

Shu, D., Ma, M., Xu, J., & Yuan, Y. (2026). The strategies to improve the survival of spray-dried probiotics: A comprehensive review. In *Food Research International* (Vol. 225). Elsevier Ltd. https://doi.org/10.1016/j.foodres.2025.118112

Sultana, A., Miyamoto, A., Lan Hy, Q., Tanaka, Y., Fushimi, Y., & Yoshii, H. (2017). Microencapsulation of flavors by spray drying using Saccharomyces cerevisiae. *Journal of Food Engineering*, *199*, 36–41. https://doi.org/10.1016/j.jfoodeng.2016.12.002

Synytsya, A., & Novák, M. (2013). Structural diversity of fungal glucans. In: *Carbohydrate Polymers* (Vol. 92, Number 1, pp. 792–809). https://doi.org/10.1016/j.carbpol.2012.09.077

Vivek, K., Mishra, S., Pradhan, R. C., Nagarajan, M., Kumar, P. K., Singh, S. S., Manvi, D., & Gowda, N. N. (2023). A comprehensive review on microencapsulation of probiotics: technology, carriers and current trends. *Applied Food Research*, *3*(1), 100248. https://doi.org/10.1016/j.afres.2022.100248

Younesi, M., Peighambardoust, S. H., Sarabandi, K., Akbarmehr, A., Ahaninjan, M., & Soltanzadeh, M. (2023). Application of structurally modified WPC in combination with maltodextrin for microencapsulation of Roselle (Hibiscus sabdariffa) extract as a natural colorant source for gummy candy. *International Journal of Biological Macromolecules*, *242*. https://doi.org/10.1016/j.ijbiomac.2023.124903

Yu, H., Kong, Q., Wang, M., Han, Z., & Xu, J. (2024). Improved viability of probiotics by encapsulation in chickpea protein matrix during simulated gastrointestinal digestion by succinylated modification. *International Journal of Biological Macromolecules*, *260*. https://doi.org/10.1016/j.ijbiomac.2024.129614

Zhang, Z., Wang, B., & Adhikari, B. (2022). Maillard reaction between pea protein isolate and maltodextrin via wet-heating route for emulsion stabilisation. *Future Foods*, *6*(September), 100193. https://doi.org/10.1016/j.fufo.2022.100193

Publisher's Note Springer Nature remains neutral with regard to jurisdictional claims in published maps and institutional affiliations.

Springer Nature or its licensor (e.g. a society or other partner) holds exclusive rights to this article under a publishing agreement with the author(s) or other rightsholder(s); author self-archiving of the accepted manuscript version of this article is solely governed by the terms of such publishing agreement and applicable law.